Acta Microscópica, Vol. 1, Nº 2, November 1992, pp 1-13

Exploratory Experiments in Convergent Beam Coherent Electron Diffraction

John W Steeds, Roger Vincent, Wendy J Vine, Paul Spellward and David Cherns
Physics Department ,University of Bristol , Bristol BS8 1TL , United Kingdom

ABSTRACT

The ability of a newly developed transmission electron microscope with a coherent source and good diffraction facilities to perform coherent electron diffraction experiments has been explored using 6H, 15R and 4H polytypes of SiC. The influence of beam coherence on convergent beam electron diffraction experiments is clearly demonstrated. A variety of different effects are presented and discussed; the prospects for future experiments are reviewed.

KEY WORDS:
convergent beam coherent electron diffraction, silicon carbide, crystal structure.

INTRODUCTION

Now that transmission electron microscopes (TEMs) are available that combine reliable field emission sources with excellent diffraction facilities, there are exciting new prospects for electron diffraction experiments at high spatial resolution. An important distinction exists, depending on the relative dimensions of the projected unit cell and the probe size. For probe sizes larger than the projected unit cell size the work which can be performed is essentially similar in character to that of conventional convergent beam electron diffraction (CBED) experiments with an incoherent source. However, the enhanced spatial resolution is of considerable importance for a number of new applications of the technique [1]. For focussed probe sizes comparable with, or smaller than, the projected unit cell size, convergent beam coherent electron diffraction (CBCED) experiments can be performed. This situation has been anticipated by work in several laboratories, but most notably in Arizona by Cowley and Spence [2,3]. However, it is only now that these ideas can be explored routinely, and the potential of the CBCED technique can be evaluated [4]. This article presents some of the first results obtained by CBCED using one of the new generation of TEMs referred to above. It is already clear that information about the relative phases of diffracted waves can be obtained straightforwardly and directly. The implications of this development are under investigation at present.

EXPERIMENTAL DETAILS

The experiments described here were performed with a Hitachi HF 2000 cold field emission transmission electron microscope operated at 200kV. A careful study was first made of the alignment and stigmation conditions which gave a symmetrical focussed probe with a FWHM of about 1 nm. Combinations of lens settings were established to give continuous variation of the convergence angle of the incident beam so as to control the degree of overlap

between diffracted beams in the electron diffraction pattern, while maintaining a well-formed probe in the specimen plane. The experimental observations were made in the diffraction plane and recorded using exposures of about 10 secs duration.

Samples of SiC were chosen for the experiments. SiC is of considerable current interest for a wide variety of applications as both a structural material and as an electronic material. It exists in a wide variety of polytypes with varying c axis repeats and it is relatively easy to obtain good samples of some of the more common polytypes. The 4H, 15R and 6H polytypes were chosen for the present experiments because the reflections along the c axis direction correspond respectively to c axis repeats (projected unit cell dimensions) of 1.0 nm, 1.25 nm and 1.5 nm.

THEORETICAL BACKGROUND

In view of the probe size and the relatively large lattice repeats explored in this work, the diffracted discs were sufficiently close together that we are able to ignore, to a first approximation, the effects of spherical aberration. We further make the assumption of thin crystals so that kinematical diffraction theory may be used, although this approximation is relaxed in the discussion of some of the results in § 5. Some of the calculations and analyses have, in fact, been performed on the basis of dynamical (Bloch wave) diffraction theory. The small diffraction angles and thin crystals also allowed us to assume, as a further simplification, constant amplitude and phase within each of the diffracted discs.

For aberration-free lenses, the form of the focussed probe on the specimen would be that of an Airy function. In the case of a single long period in the projected unit cell, the problem can be reduced effectively to one dimension (x). Suppose the condenser aperture and lens settings cause an angular convergence of 2K/k within the incident probe of wave number k(=2π/λ) then, in one dimension, the intensity distribution in the probe would be $\sin^2 Kx / K^2x^2$, with a first minimum of intensity at $x = \pi / K$. If the long period repeat is d, then the corresponding separation of diffraction maxima is $g = 2\pi/d$ and for overlaps of diffraction discs we require $2K > g$. It follows from this condition that $d > \pi/K$, or that the probe size must be comparable with or less than the projected cell size for overlap to occur and CBCED to take place.

For the case of a focussed probe on the specimen a common point in the overlap region between two reflections g_1 and g_2 will combine wave amplitudes with identical path lengths from the specimen to that point (Fig 1).

The coherent addition of wave amplitudes A_1 and A_2 from the two reflections will give rise to an intensity (I) in the overlap region, where

$$I = A_1A_1^* + A_2A_2^* + A_1A_2^* + A_2A_1$$

For kinematical diffraction we have (omitting constants of proportionality)

$$A_1 = F_1 e^{i(\phi_1 + \underline{g}_1 \cdot \underline{R})}$$
$$A_2 = F_2 e^{i(\phi_2 + \underline{g}_2 \cdot \underline{R})}$$

where F_1, F_2 are the amplitudes and ϕ_1, ϕ_2 are the phases of the structure factors corresponding to the reflections g_1, g_2 and $\underline{R} = (x,y)$ describes the probe position within the projected unit cell.

It follows that

$$I = F_1^2 + F_2^2 + 2F_1F_2\cos(\phi_2 - \phi_1 + gx)$$

where $g = 2\pi/d = |\underline{g}_2 - \underline{g}_1|$ and x describes the probe position relative to the one-dimensional cell of period d. The overlap intensity depends, therefore, on the relative phases of the two structure factors, and varies with period d as the probe is moved to attain a maximum value

$$I_{max} = F_1^2 + F_2^2 + 2F_1F_2$$

and a minimum value

$$I_{min} = F_1^2 + F_2^2 - 2F_1F_2$$

If the beam crossover is adjusted slightly from the plane of the specimen by a defocus, Δf, of the probe forming lenses, the phase origin becomes orientation-dependent (Fig. 2). Different angles of incidence within the incident beam correspond to different phase origins and the shift of origin is given by $\Delta x \approx K\Delta f/k$. When K

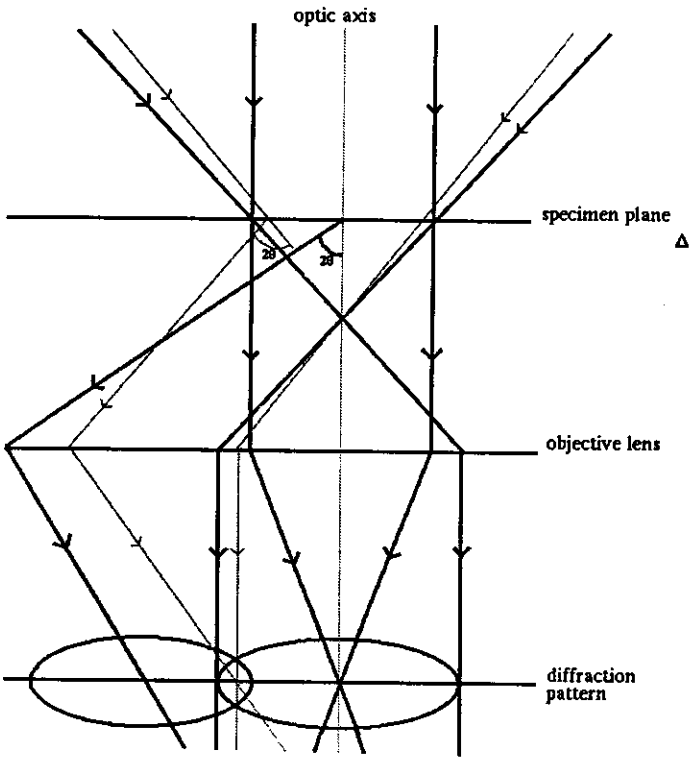

Fig. 1 Schematic ray diagram for in-focus convergent coherent beam electron diffraction experiments.

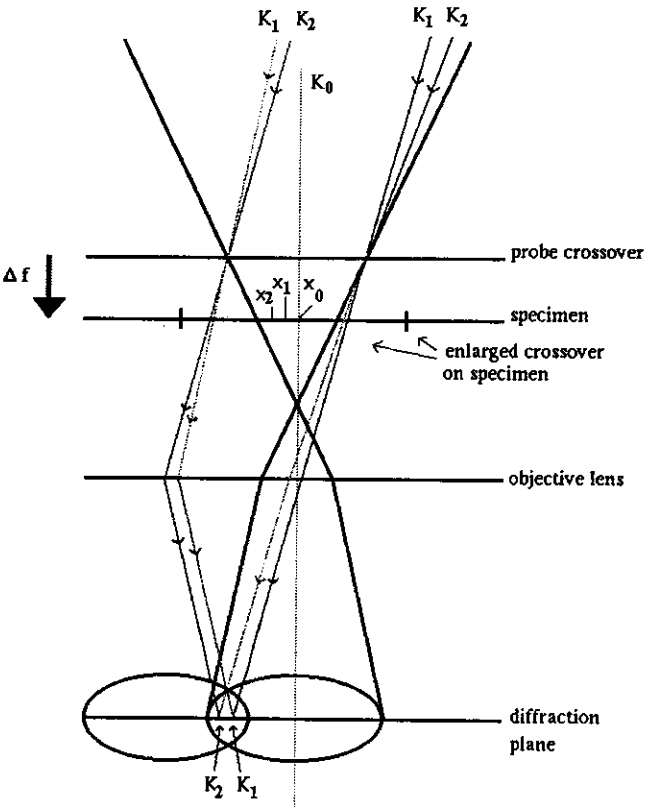

Fig. 2 Schematic ray diagram for out-of-focus convergent coherent beam electron diffraction experiments, illustrating that different orientations in the region of overlap between diffracted discs have different phase origins (x_0, x_1 and x_2 corresponding to K_0, K_1 and K_2).

defines position in the diffraction plane and K/k is the angle of propagation relative to the optic axis. It follows that the new expression for the intensity in the region of overlap is given by

$$I = F_1^2 + F_2^2 + 2F_1F_2\cos[\phi_2 - \phi_1 + g(x + K\Delta f/k)]$$

Hence, the overlap region is filled with fringes perpendicular to the line joining g_2 to g_1 (ie g) and the fringe spacing decreases as Δf increases. The visibility of these fringes is given by the expression

$$V = I_{max} - I_{min} / I_{max} + I_{min} = 2F_1F_2 / F_1^2 + F_2^2$$

For $F_1 \approx F_2$ the fringe visibility is therefore approximately unity, but for $F_1 >> F_2$ the visibility is $2F_2/F_1$

EXPERIMENTAL RESULTS

(a) Beam focussed on the specimen

Experiments were first performed on the 6H polytype of SiC at the <11$\bar{2}$0> zone axis. With the convergence angle chosen for overlap between the reflections in the systematic rows, such as (1$\bar{1}$0n), parallel to c*, position-dependent intensity was observed in the overlap region. In fact the sensitivity to the probe position was so great that even the slight degree of instability present in the focussed probe was sufficient to give flickering overlap intensity for a 'stationary' probe. Rather than obtain time averaged diffraction patterns, the height of the probe crossover was adjusted by a small defocus of the first condenser lens

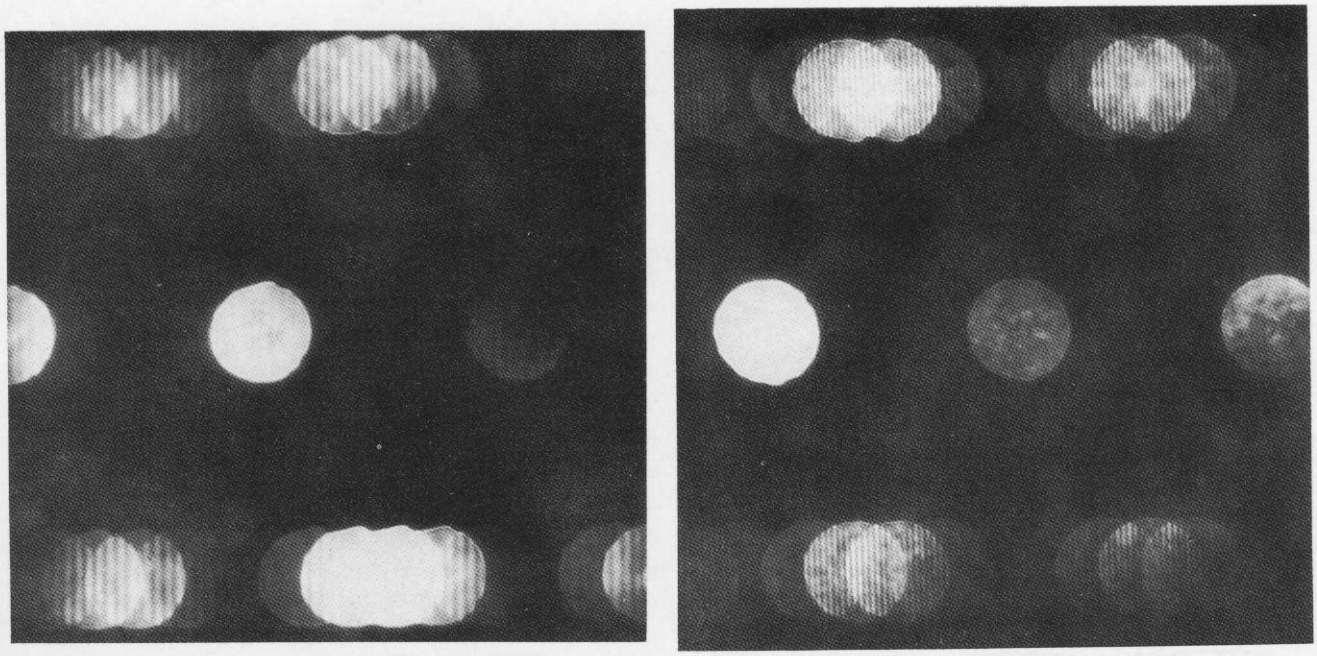

Fig. 3 Experimental results obtained at 200kV on <11$\bar{2}$0> 6H Sic, illustrating the reduction of fringe spacing in the overlap region between adjoining diffraction discs with increase of condenser lens over-focus.

(b) Over-focussed beam

In the over-focussed condition, sets of parallel fringes were obtained in the region of overlap between adjoining diffraction discs. As the degree of over-focus was progressively increased, the fringes came ever closer together until they were no longer visible (Fig. 3). At present, a maximum of about twelve fringes has been observed in the overlap between reflections from the 6H polytype. As the projected unit cell has a c axis period of 1.5 nm, this corresponds to a probe size on the specimen of about 36 nm.

Careful study of the fringe patterns obtained in this way revealed several interesting features. Along any chosen systematic row such as (1$\bar{1}$0n), ($\bar{1}$10n), ($\bar{2}$20n) etc the fringe patterns observed in different overlap regions were found to have different phasings. The phasing of the fringes can be characterized by observing their location relative to a reference point such as the common line of intersection of two neighbouring discs. Successive systematic rows showed a phase slip of approximately π relative to adjoining rows. Rows related by a mirror operation through the central line of the reflections (000n) were also apparently π out of phase with respect to each other. This behaviour, first noted for the 6H

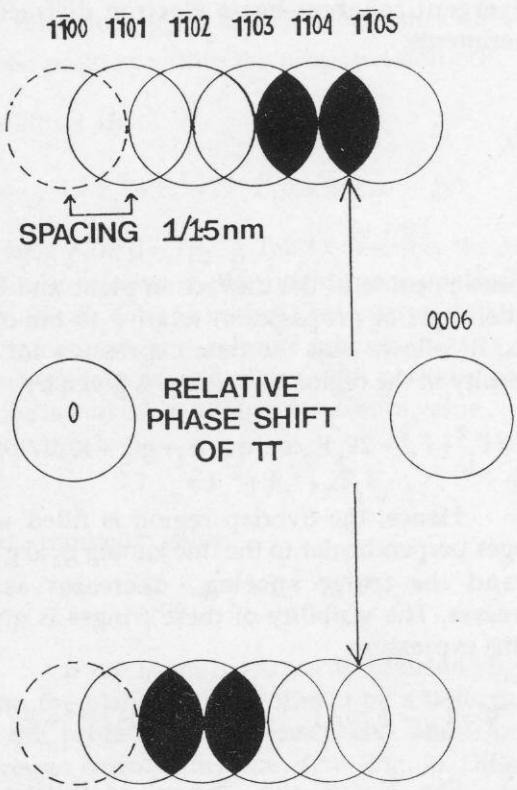

Fig. 4 Schematic diagram to indicate the indexing of reflections in Fig 3.

polytype, was also reproduced in later experiments on the 4H polytype. It should also be noted that the behaviour described above and illustrated schematically in Fig. 4 breaks the mirror line normally seen parallel to c* in conventional CBED experiments. The CBCED patterns from the 15R polytype also showed phase shifts of fringes along the systematic rows, but as the reflections do not lie in mirror-related positions on either side of c*, the phase relationship between related systematic rows is altered from that of 6H and 4H polytypes.

During the course of the experiments summarized above, it was noted that fringes sometimes deviated from their expected orientation. Two different types of deviation have been distinguished with essentially different origins.

We shall first discuss the situation, evident in Fig. 5(a), where the fringes in every region of overlap are parallel to each other but no longer parallel to the common line of intersection of adjoining discs. A series of experiments was performed on the 4H polytype with systematic adjustment of the second order condenser stigmator control of an otherwise well-corrected probe. It was found that this control caused the fringes to rotate in orientation, as indicated in Fig. 6. By gross misadjustment, fringes approximately perpendicular to the expected orientation could be obtained.

A second effect, illustrated in Fig. 5(b), gave rise to different fringe orientations in different overlap regions. As this effect was only observed in rather thick regions of the specimen, it seems likely that it was caused by changes of the phase angle introduced within the region of overlap by dynamical diffraction effects.

The results described above were obtained from 6H, 15R and 4H polytypes, and the fact that the c repeat in the 4H polytype is 1 nm indicates that the 1 nm probe produced by the instrument is reasonably coherent. However, the clearest fringes were obtained from the 6H polytype with a 1.5 nm c axis repeat distance. As further test, the convergence angle was increased so as to cause the $(1\bar{1}01)$ and $(11\bar{0}1)$ reflections of the 6H polytype to overlap. As the $(1\bar{1}00)$ reflection is absent under conditions of kinematical diffraction, the overlap of next nearest neighbour discs could be observed without the complication of nearest neighbour overlaps. The result is illustrated in Fig. 7 and careful examination reveals fringes in the region of overlap with twice the spatial frequency (0.75 nm).

An interesting observation, closely related to the 4H and 6H phase change of between mirror-related positions either side of c*, was made in the (000n) systematic row from thick regions of the 6H polytype. If the specimen was accurately aligned, the fringes in the overlap regions in this row were no longer continuous and parallel but had a reasonably abrupt phase change of π along the line of symmetry (Fig 8).

All the observations reported so far have been made on reflections in the zero layer plane of the $[11\bar{2}0]$ zone axis. Can such effects be observed in other Laue zones? By careful choice of specimen thickness it was possible to record diffraction patterns at the $<10\bar{1}0>$ zone axis with ten second exposures having appreciable first order Laue zone (FOLZ) intensities. When this was achieved, the resulting negatives revealed that the FOLZ ring was modulated with fringes parallel to the c axis repeat (Fig 9). Change of defocus changed the fringe spacing.

DISCUSSION OF RESULTS

The experimental results which have been obtained indicate clearly that CBCED is capable of giving the relative phases of diffracted waves. To examine this point more thoroughly, computations were performed on the basis of the theoretical background described in § 2, using dynamical rather than kinematical diffraction theory. Fig. 10, shows the calculated results for a 5 nm thick 6H SiC specimen at zero defocus and two other defocus settings. The superficial similarity between these computed results and the experimental micrographs is evident. In order to overcome the difficulty of assessing the relative phases of fringes in the overlap regions, the phasings have been shown explicitly in Fig 11. The central vertical line in the graphs represents the common line of intersection of neighbouring discs. The lefthand side of the graph corresponds to the top of the appropriate overlap region. From the complicated pattern of phasings one can note the π phase change in mirror-related reflections

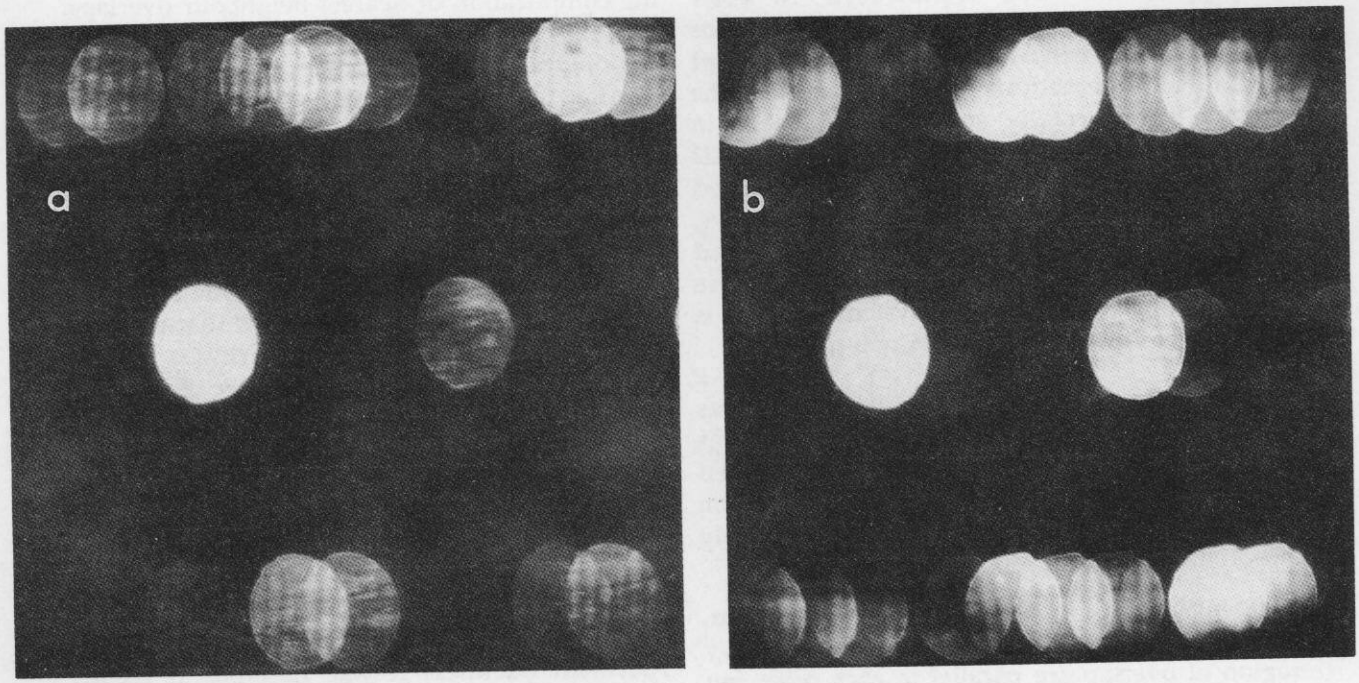

Fig. 5 Rotation of fringes from their expected orientation in <11$\bar{2}$0> 15R SiC, at 200kV. In (a) the fringes are all in the same orientation, while in (b) taken from a much thicker region of the specimen, the fringe rotation varies from place to place.

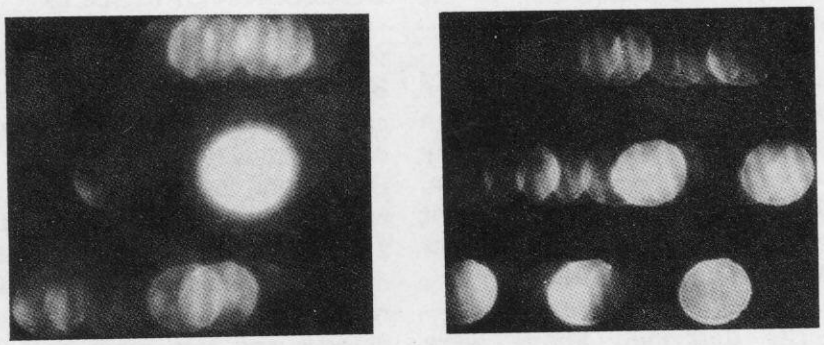

Fig. 6 Fringe rotation experiments performed at 200kV using <11$\bar{2}$0> 4H SiC, illustrating the change in sense of rotation with change in the condenser stigmator setting.

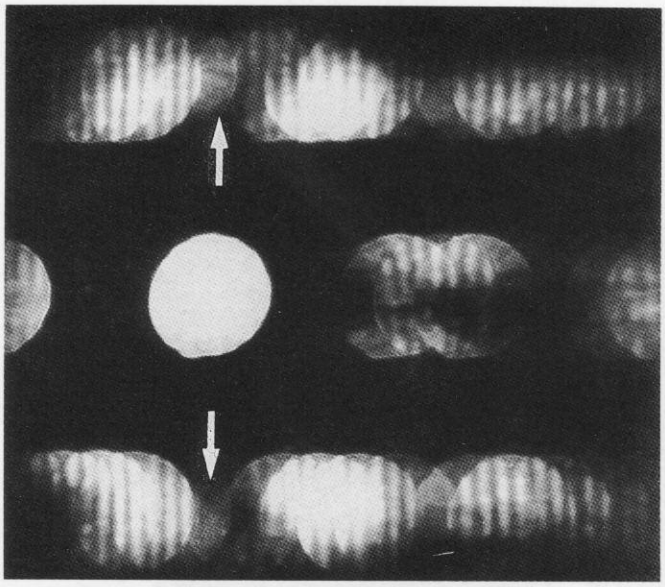

Fig. 7 Second order disc overlap between the $(1\bar{1}01)$ and $(1\bar{1}0\bar{1})$ reflections of <11$\bar{2}$0> 6H SiC at 200kV. Very fine fringes may just be observed with half the spacing of those in the first order overlaps.

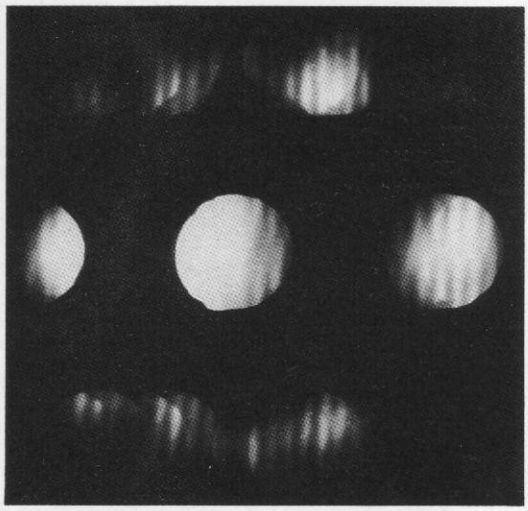

Fig. 8 <11$\bar{2}$0> 6H SiC illustrate a π phase change across the centre of the three strong reflections at the middle of the diffraction pattern.

either side of c*, and a further phase change of π in the first set of overlap fringes above and below a horizontal line through the centre of the pattern.

Computations performed for a crystal thickness of 50 nm show superficially similar results (Fig 12), but the phasings of fringes in the overlap regions is altered, different overlaps experiencing phase changes of different magnitude. However, the π phase change either side of the mirror line parallel to c* is preserved, as is the π change immediately above and below a horizontal line through the centre of the pattern. The results in Fig 12 also show new features of low visibility in reflections where no contrast was apparent in Fig 11. In order to bring out this detail, Fig 12 has been redisplayed with enhanced contrast for some of the overlaps along the c* direction in Fig 13. The π phase shift of fringes along the central line, which was noted in Fig 8 and discussed earlier, is now clearly visible. This effect, which is the result of the glide plane parallel to the zone axis direction and intersecting the pattern along c*, takes the place of the well-known Gjønnes Moodie lines [5] in the case of incoherent CBED. The glide plane is also the explanation for the π phase shift in reflections related by reflection in the mirror line along c*. The CBCED patterns now show true symmetry, in the sense that the glide plane is a composite operation involving a mirror reflection and translation, and the pattern symmetry is consistent with this composite operation

It is clear that accurate measurements are required, in order to take advantage of all the information about pairwise relative phase shifts between diffracted waves which are recorded in a single electron micrograph throughout the zero layer and FOLZs of these patterns. The fineness of the fringes which have been recorded either by large defocus (Fig 3) or by second order overlaps (Fig 7) indicates that. We are now in the process of determining the accuracy to which phase angles may be determined by digitisation of the CBCED patterns. An example of a digitised region of a pattern, together with a line scan through the pattern centre, is shown in Fig 14. Better fringe definition could be achieved in the future by averaging along the lines of the fringes, but it is already apparent that a phase change of about $\pi/10$ is detectable.

The question arises as to the use of the phase information which can be obtained by CBCED. It follows directly from the results presented here that lines of overlapping

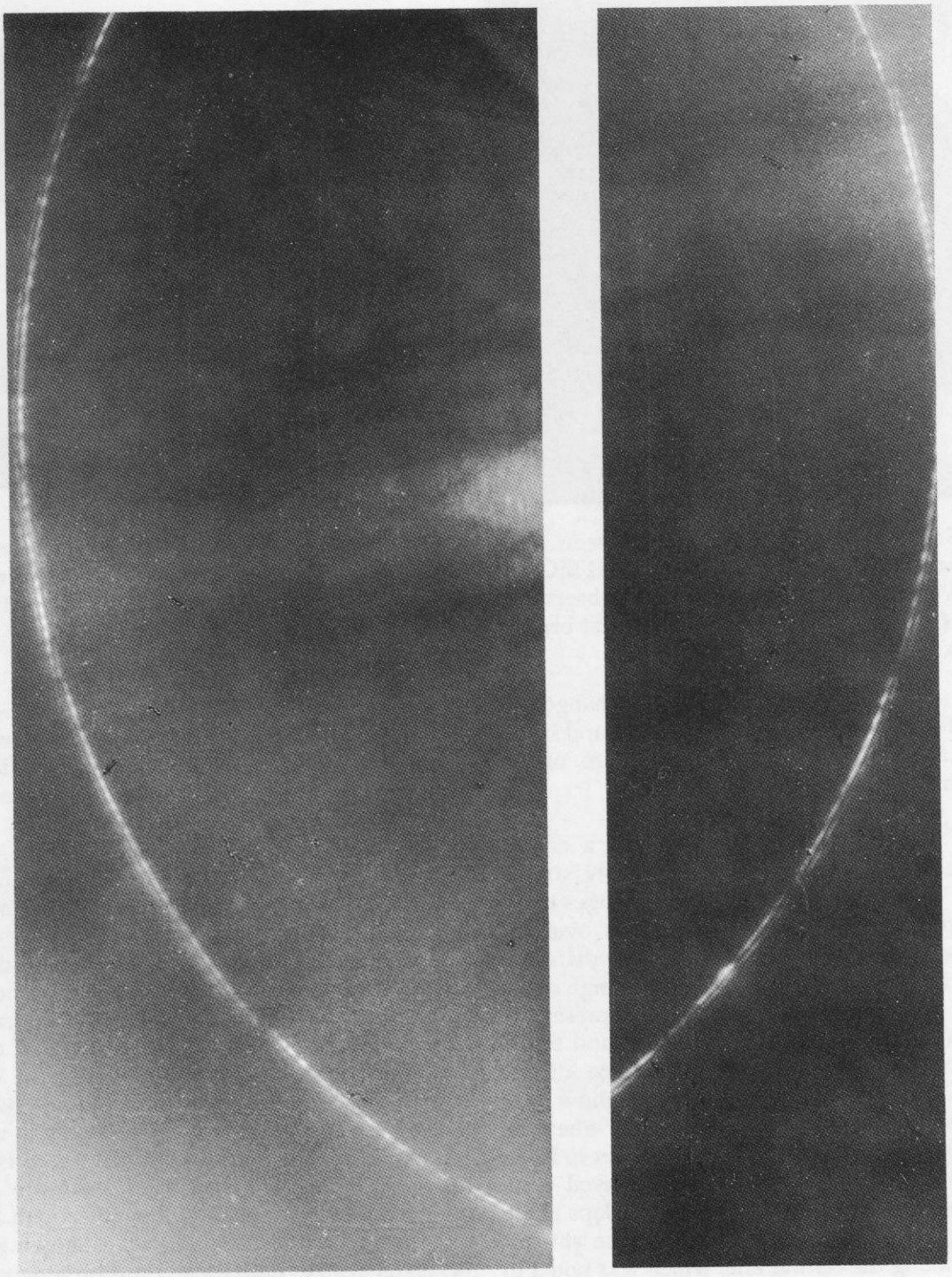

Fig. 9 Interference fringes visible in segments of the first order Laue zone of the <10$\bar{1}$0> zone axis of 6H SiC at 200kV.

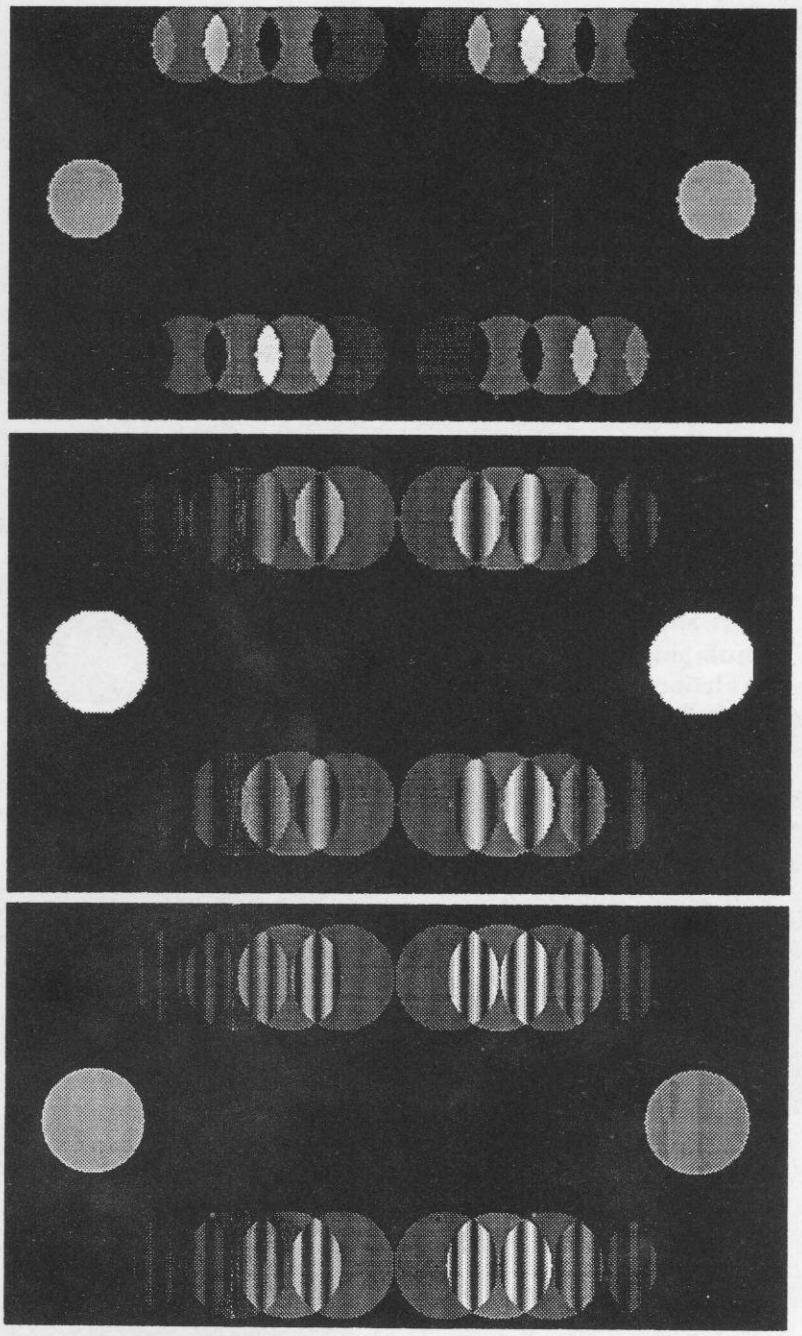

Fig. 10 Simulated convergent coherent beam electron diffraction patterns for a focussed probe (top) and two different defocus values.

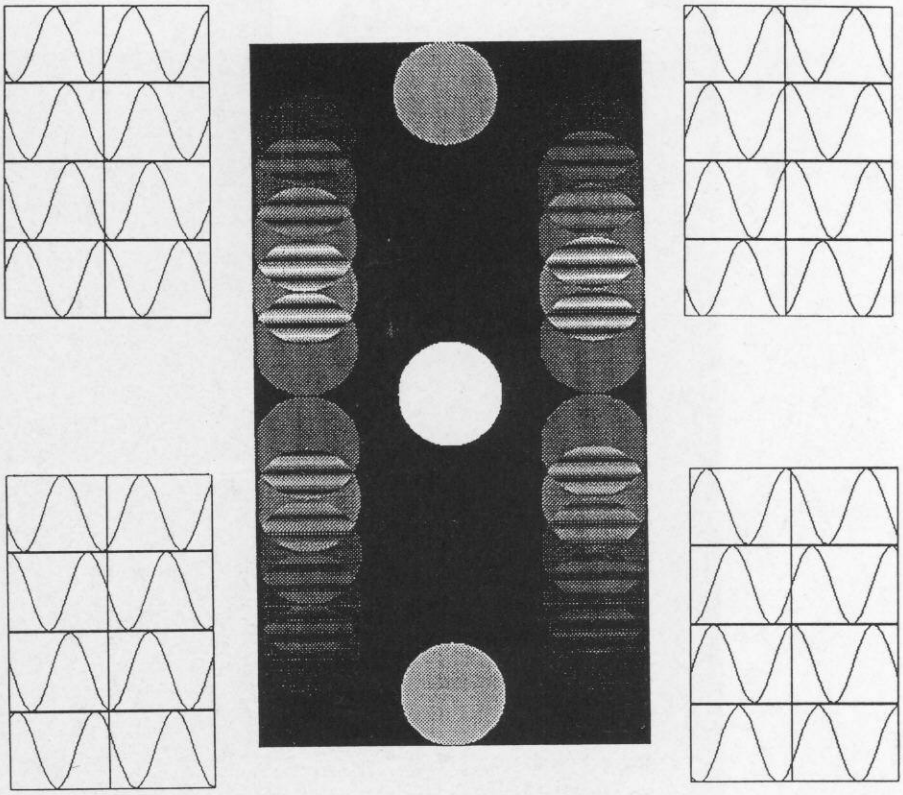

Fig. 11 Diagrams to illustrate the phasing of the fringes in the eight strong disc overlaps to left and right of the central simulated diffraction pattern. The simulation is for the <11$\bar{2}$0> axis of 5 nm thick SiC at 200kV.

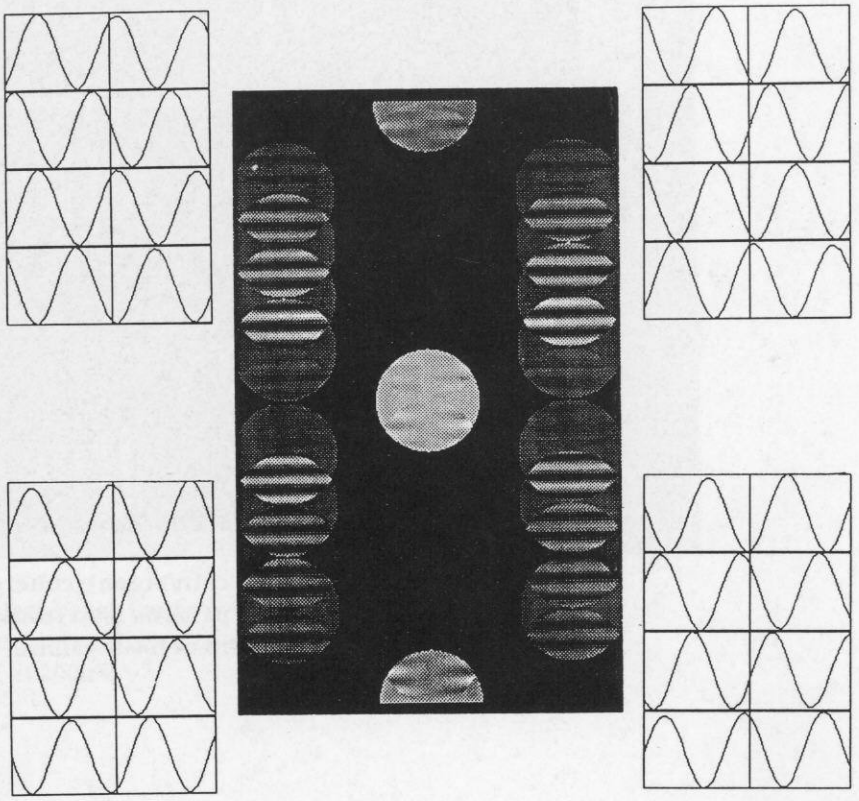

Fig. 12 The sames as for Fig 11, except that the sample thickness is now 50 nm, so that dynamical diffraction effects are important, and the phasing of the fringes in the overlap region is therefore changed.

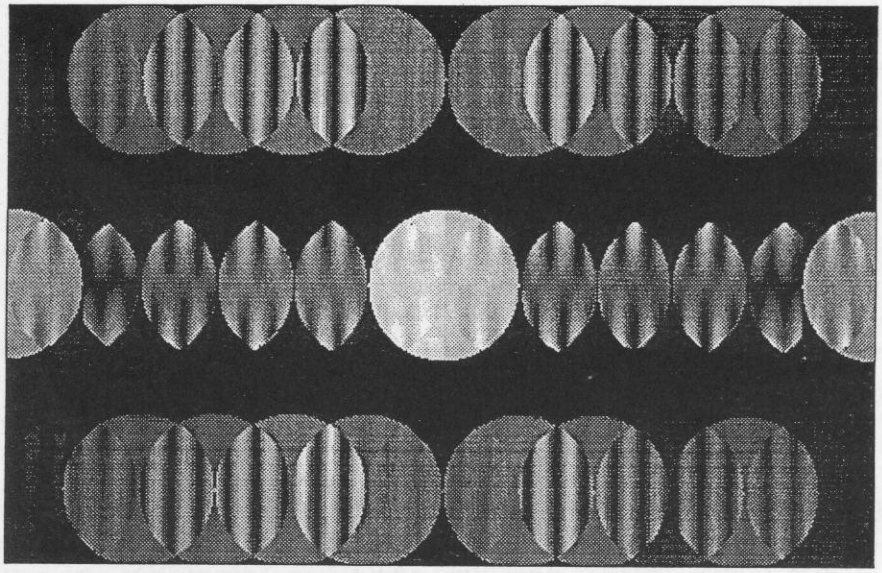

Fig. 13 Computer enhancement of pattern detalil along the middle line of reflections. The pattern is the same as that of Fig 12 after a rotation of 90°.

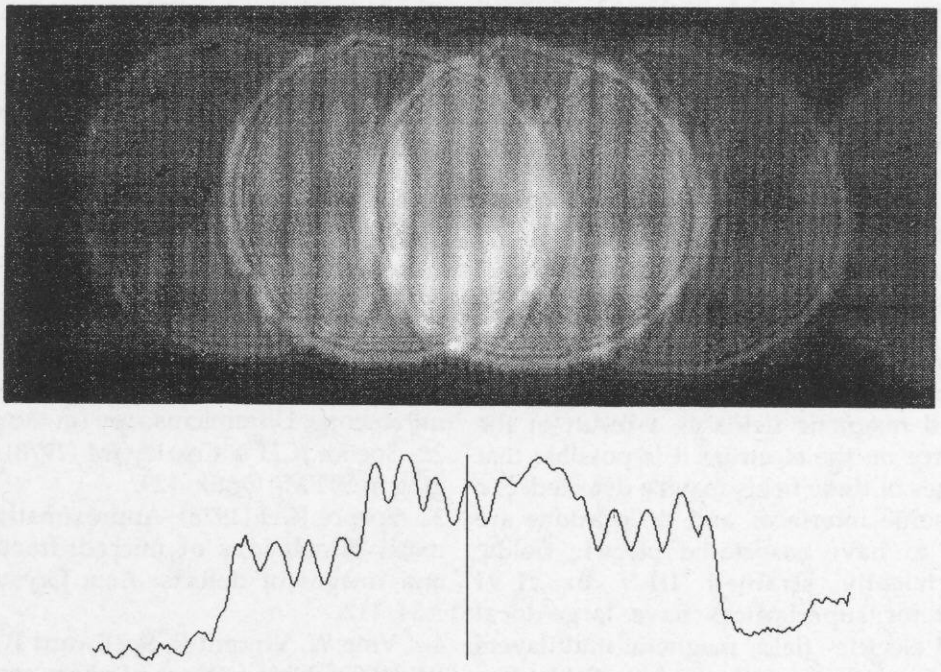

Fig 14 Digitised overlapping row of convergent beam diffraction discs for <11$\bar{2}$0> 6H SiC at 200kV, and a line profile of intensity along the central line of the digitised region.

diffraction discs can be used to determine the relative phases of the associated diffracted waves. In order to extend this to the zero layer plane, coherent two-dimensional overlap is required. If the crystal studied is thin enough, the relative phases are those of the structure factors associated with the reflections. However, dynamical effects and curvature of the Ewald sphere mean that such a simple relationship will not occur in general. It may be that the occurrence of dynamical diffraction between adjacent lines of overlapping reflections will permit their relative phasing. The example illustrated here (Figs 8 and 13) of double diffraction into kinematically forbidden reflections is a case in point. Double diffraction between the HOLZs and the ZOLZ may help to relate relative phases determined in a HOLZ ring to the zero layer plane phasing. Alternatively, the fact that, to a first approximation, HOLZ fine structure is a consequence of HOLZ dispersion sphere intersection of the zero layer dispersion surface may be sufficient to relate the phasings in the two planes. There is some experimental evidence in the existing results that the phasing of different branches of the HOLZ fine structure varies from branch to branch.

It will be interesting in the future to extend these studies to dislocations, interfaces and grain boundaries which can be directly resolved in the out-of-focus CBCED mode of operation. There are exciting prospects for obtaining new information about the atomic structure in the local area of interest at a resolution determined by the focussed probe size. In addition, since the phase will be sensitive to electric and magnetic fields as a result of the Lorentz force on the electron, it is possible that local changes of these fields may be detected. For example, some interfaces and dislocations are believed to have associated electric fields; piezo-electrically strained III-V or II-VI semiconductor superlattices have large local changes of electric field, magnetic multilayers have large local changes of magnetic fields, free edges of specimens have very strong local electric fields, and may also have longer range changes of electric or magnetic field. Recent experiments by electron holography have already detected some of these effects [6]. Future experiments will reveal what can be achieved by CBCED.

CONCLUSIONS

Convergent beam coherent electron diffraction experiments have been performed on three polytypes of SiC. The results indicate that the relative phases of diffracted waves may be determined along systematic rows of overlapping reflections for projected unit cell sizes of down to at least 1 nm. The lower limit of the projected cell dimensions for which the experiments can be performed has still to be determined. Observations may be made in both the zero layer and HOLZs at a given zone axis. The relative phasing of different systematic rows may be used to deduce the presence of glide planes in the crystal structures. The symmetries of the patterns are changed from those of conventional CBED experiments to more accurately represent the true symmetry properties of crystals under investigation. The question of the experimental accuracy of phase angle measurement needs to be resolved, and this will determine the extent to which the results presented here can be used in crystallographic investigations, defect and interface studies, and the examination of local electric and magnetic fields.

ACKNOWLEDGEMENTS

The authors wish to thank SERC for financial support of this project, and one of us (Wendy Vine) also wishes to thank Rolls Royce plc for financial support.

REFERENCES

1. Steeds JW & Vincent R (1992). Prospects for convergent beam electron diffraction with a 200kV cold field emission transmission electron microscope. Ultramicroscopy (in the press).
2. Spence JCH & Cowley JM (1978). Lattice imaging in STEM. Optik, 129.
3. Spence JCH (1978). Approximations for dynamical calculations of microdiffraction patterns and images of defects. Acta Crystallographica A34, 112.
4. Vine W, Vincent R, Spellward P & Steeds JW (1992). Observations of phase contrast in convergent-beam electron diffraction patterns. Ultramicroscopy, 41: 423.
5. Gjønnes J & Moodie A F (1965). Extinction conditions in the dynamic theory of electron diffraction. Acta Crystallographica 19,65.
6. Kawasaki T, Ru QX, Matsuda T & Tonomura

A (1991). Electron holography of crystal structure image. Institute of Physics Conference Series No. 119, Electron Microscopy and Analysis 1991, Institute of Physics, Bristol, Philadelphia & New York, 483.